

Tufted Cell Dendrodendritic Inhibition in the Olfactory Bulb Is Dependent on NMDA Receptor Activity

J. M. Christie, N. E. Schoppa and G. L. Westbrook
J Neurophysiol 85:169-173, 2001.

You might find this additional information useful...

This article cites 25 articles, 11 of which you can access free at:

<http://jn.physiology.org/cgi/content/full/85/1/169#BIBL>

This article has been cited by 2 other HighWire hosted articles:

Mitral and Tufted Cells Differ in the Decoding Manner of Odor Maps in the Rat Olfactory Bulb

S. Nagayama, Y. K. Takahashi, Y. Yoshihara and K. Mori
J Neurophysiol, June 1, 2004; 91 (6): 2532-2540.

[\[Abstract\]](#) [\[Full Text\]](#) [\[PDF\]](#)

Dendrodendritic Inhibition and Simulated Odor Responses in a Detailed Olfactory Bulb Network Model

A. P. Davison, J. Feng and D. Brown
J Neurophysiol, September 1, 2003; 90 (3): 1921-1935.

[\[Abstract\]](#) [\[Full Text\]](#) [\[PDF\]](#)

Medline items on this article's topics can be found at <http://highwire.stanford.edu/lists/artbytopic.dtl> on the following topics:

Oncology .. N-Methyl-D-Aspartate Receptors
Biochemistry .. Aspartate
Veterinary Science .. Olfactory Bulb
Physiology .. Smell
Physiology .. Glomerulus
Medicine .. Kidney Glomerulus

Updated information and services including high-resolution figures, can be found at:

<http://jn.physiology.org/cgi/content/full/85/1/169>

Additional material and information about *Journal of Neurophysiology* can be found at:

<http://www.the-aps.org/publications/jn>

This information is current as of April 3, 2007 .

Tufted Cell Dendrodendritic Inhibition in the Olfactory Bulb Is Dependent on NMDA Receptor Activity

J. M. CHRISTIE, N. E. SCHOPPA, AND G. L. WESTBROOK

Vollum Institute, Oregon Health Sciences University, Portland, Oregon 97201

Received 13 June 2000; accepted in final form 29 September 2000

Christie, J. M., N. E. Schoppa, and G. L. Westbrook. Tufted cell dendrodendritic inhibition in the olfactory bulb is dependent on NMDA receptor activity. *J Neurophysiol* 85: 169–173, 2001. Mitral and tufted cells constitute the primary output cells of the olfactory bulb. While tufted cells are often considered as “displaced” mitral cells, their actual role in olfactory bulb processing has been little explored. We examined dendrodendritic inhibition between tufted cells and interneurons using whole cell voltage-clamp recording. Dendrodendritic inhibitory postsynaptic currents (IPSCs) generated by depolarizing voltage steps in tufted cells were completely blocked by the *N*-methyl-D-aspartate (NMDA) receptor antagonist D,L-2-amino-5-phosphonopentanoic acid (D,L-AP5), whereas the α -amino-3-hydroxy-5-methyl-4-isoxazolepropionic acid (AMPA) receptor antagonist 2,3-dioxo-6-nitro-1,2,3,4-tetrahydrobenzo[f] quinoxaline-7-sulfonamide (NBQX) had no effect. Tufted cells in the external plexiform layer (EPL) and in the periglomerular region (PGR) showed similar behavior. These results indicate that NMDA receptor-mediated excitation of interneurons drives inhibition of tufted cells at dendrodendritic synapses as it does in mitral cells. However, the spatial extent of lateral inhibition in tufted cells was much more limited than in mitral cells. We suggest that the sphere of influence of tufted cells, while qualitatively similar to mitral cells, is centered on only one or a few glomeruli.

INTRODUCTION

The two classes of primary output neurons in the main olfactory bulb, mitral cells and tufted cells, share several common features. Each receives sensory input from olfactory nerve axons in the neuropil of the glomerular layer and in turn project their axons to piriform cortex. Within the bulb, dendrodendritic synapses form between interneurons and the primary and secondary dendrites of both mitral and tufted cells. Mitral cells are located in a compact layer referred to as the mitral cell layer (MCL), whereas tufted cells are dispersed throughout the external plexiform layer (EPL) and the periglomerular region (PGR) (Cajal 1911). Tufted cells are also considerably more diverse in their morphology (Scott and Harrison 1991).

Our understanding of olfactory bulb function is largely based on studies of mitral cells and the dendrodendritic synapses between mitral and granule cells. At this unique synapse, release of glutamate from mitral cell dendrites drives GABA release from granule cells that then leads to recurrent and lateral inhibition of mitral cells. Dendrodendritic inhibition of mitral cells can be quite prolonged and follows the slow

kinetics of *N*-methyl-D-aspartate (NMDA) receptors on granule cells (Mori and Takagi 1978; Schoppa et al. 1998). Dendrodendritic inhibition provides the first step in the network processing of odorant responses that are mapped onto glomeruli in a highly ordered manner (Vassar et al. 1994). As a result, the duration and spatial extent of GABAergic inhibition is likely to have a major impact on sensory integration.

The role of tufted cells in olfactory processing is not well characterized, but there is reason to think their function is distinct from mitral cells. For example, the distribution of dendrites in the bulb suggests that the dendrites of principal cells may preferentially interact with different sets of interneurons. Granule cell dendrites are present either in the deep zones of the EPL where secondary mitral cell dendrites are located, or in more superficial zones of the EPL where tufted cell secondary dendrites are located (Mori et al. 1983; Orona et al. 1983). Furthermore, dendrodendritic synapses of tufted cells in the PGR may be restricted to periglomerular cell interneurons (Pinching and Powell 1971a; Price and Powell 1970a,b). Distinct interneuronal circuits may also underlie the differences in inhibitory postsynaptic potential (IPSP) size in these two types of principal cells (Ezeh et al. 1993). We examined dendrodendritic inhibition in tufted cells in both the EPL and PGR using whole cell recording from slices of young rats. Tufted cells were identified visually by their location; morphological subtypes were classified using intracellular dye injections.

METHODS

Slices of the main olfactory bulb (400 μ M) were prepared from Sprague-Dawley rat pups [*postnatal day 10 to 14 (P10–P14)*] as described (Schoppa et al. 1998). Tufted cells, visualized by infrared DIC optics, were identified by location and morphology (Scott and Harrison 1991). All experiments were performed at room temperature (21–24°C). Whole cell voltage-clamp recordings were made in an oxygenated, magnesium-free solution containing (in mM) 125 or 140 NaCl, 25 NaHCO₃, 25 glucose, 2.5 KCl, 1.25 NaH₂PO₄, and 2 CaCl₂, pH 7.3. Patch pipettes (4–8 M Ω) were filled with an intracellular solution containing (in mM) 140 KCl, 10 EGTA, 10 HEPES, 2 MgCl₂, 2 CaCl₂, 2 NaATP, and 0.5 NaGTP, pH 7.3. In some cases, tufted cells were filled with the dye Alexa 568 hydrazide (Molecular Probes, Eugene, OR; 0.1 mg/ml) and visualized after fixation using confocal microscopy (Odyssey XL, Noran Instruments, Middleton, WI). To verify the location of tufted cell dendrites, slices were

Address for reprint requests: J. M. Christie, Vollum Institute, Oregon Health Sciences University, 3181 SW Sam Jackson Park Rd., Portland, OR 97201 (E-mail: christij@ohsu.edu).

The costs of publication of this article were defrayed in part by the payment of page charges. The article must therefore be hereby marked “advertisement” in accordance with 18 U.S.C. Section 1734 solely to indicate this fact.

counterstained with the nucleic acid stain SYTO-13 (1:4,000, Molecular Probes, Eugene, OR).

To evoke dendrodendritic inhibitory postsynaptic currents (IPSCs), a depolarizing voltage step (0 mV, 5 ms) was applied to the soma of a voltage-clamped tufted cell. To examine lateral inhibition, IPSCs were evoked by stimulating the glomerular layer with a tungsten electrode (0.5 M Ω , WPI, Sarasota, FL) centered on a single glomerulus. Stimulation pulses (100 V, 100 μ s) were generated by a stimulation isolation unit (Winston Electronics, Millbrae, CA). IPSCs were recorded with an Axopatch 1B (Axon Instruments, Foster City, CA), filtered with the built-in 4-pole Bessel filter and digitized at 2 kHz. Access resistance (R_s) was constantly monitored; recording was terminated when R_s was >15 M Ω . All data were analyzed using AXOGRAPH (Axon Instruments). IPSC charge was estimated by integrating the baseline-subtracted current. Statistical significance was determined using standard Student's *t*-tests or repeated measures ANOVA as appropriate (Microsoft Excel, Redmond, WA).

RESULTS

Dendrodendritic inhibition in tufted cells is driven by NMDA receptors

We first examined tufted cells with cell bodies located in the intermediate zone of the EPL (Fig. 1A). In whole cell voltage clamp, a depolarizing voltage step (0 mV, 5 ms) elicited a

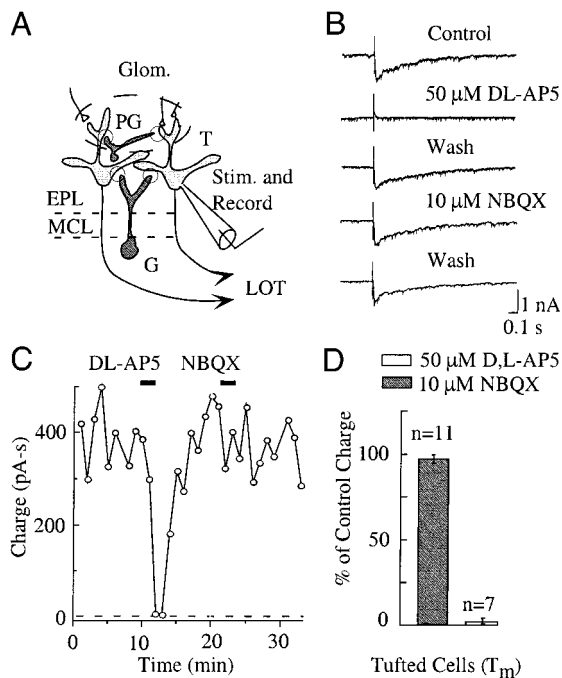


FIG. 1. *N*-methyl-D-aspartate (NMDA) receptor activation is required for dendrodendritic inhibition in tufted cells (T_m) in the external plexiform layer (EPL) of the olfactory bulb. *A* and *B*: a tufted cell in the EPL was voltage clamped at -70 mV. Depolarizing voltage steps (5 ms, to 0 mV) triggered glutamate release from tufted cell dendrites and activation of synaptically coupled granule cells (G) and/or periglomerular cells (PG). The resulting GABA release caused an inhibitory postsynaptic current (IPSC) in the tufted cell. This was recorded as a slow inward GABA_A current in the chloride-loaded tufted cell. The IPSC was completely blocked by D,L-2-amino-5-phosphonopentanoic acid (D,L-AP5; 50 μ M), but not by 2-3-dioxo-6-nitro-1,2,3,4-tetrahydrobenzo[f] quinoxaline-7-sulfonamide (NBQX) (10 μ M). Each trace is an average of several trials. *C* and *D*: the reduction in charge (pA-s) by AP5 was completely reversible as shown for the same cell as in *B*. Summary data for 13 intermediate tufted cells is shown in *D*. Charge values were generated by integrating the reciprocal IPSC. LOT, lateral olfactory tract; MCL, mitral cell layer.

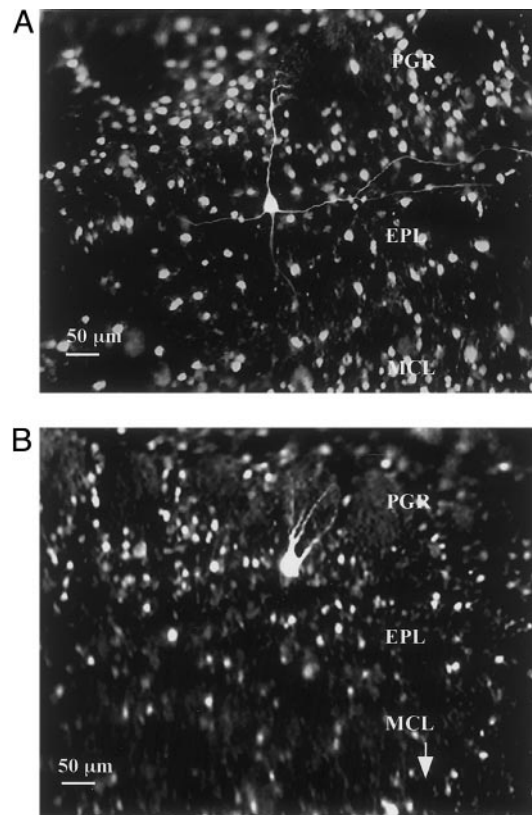


FIG. 2. Tufted cells filled with Alexa 568 hydrazide illustrate the distinct morphologies of tufted cells. *A*: a tufted cell with soma located in the external plexiform layer (EPL) had a single primary dendrite that projected into the periglomerular region (PGR) and secondary dendrites that extended laterally in the EPL. The process extending toward the mitral cell layer is the presumptive axon. *B*: tufted cell with soma in PGR had a branched primary dendrite extending locally in the PGR, but no apparent laterally projecting secondary dendrites. The axon in this cell is not visualized in this image. The margins of glomeruli were visualized by staining with the nucleic acid marker SYTO-13 that labeled the cell bodies of interneurons and glia surrounding each glomerulus.

slowly decaying IPSC due to activation of dendrodendritic synapses. Bath application of bicuculline methiodide (40 μ M) completely blocked the IPSC, consistent with activation of GABA_A receptors ($5 \pm 2.9\%$ of control, mean \pm SE, $n = 3$). The selective NMDA receptor antagonist D,L-2-amino-5-phosphonopentanoic acid (D,L-AP5; 50 μ M) completely and reversibly abolished the IPSC, whereas the α -amino-3-hydroxy-5-methyl-4-isoxazolepropionic acid (AMPA) receptor antagonist 2-3-dioxo-6-nitro-1,2,3,4-tetrahydrobenzo[f] quinoxaline-7-sulfonamide (NBQX) (10 μ M) had no effect (Fig. 1, *B–D*). The dependence of dendrodendritic inhibition on NMDA receptor activation is also observed in mitral cells under the same conditions (see Schoppa et al. 1998). The amplitude and time course of the IPSCs were similar to those recorded in mitral cells (not shown) (see Schoppa et al. 1998).

As for mitral cells, dendrodendritic inhibition of tufted cells may occur either on primary dendrites in the glomerular layer or on secondary dendrites in the EPL (Macrides and Schneider 1982; Mori et al. 1983; Orona et al. 1984). However, tufted cells can be subtyped into three groups based on their somatic location and dendritic arbors (Scott and Harrison 1991): T_s , soma and dendrites in the superficial EPL; T_m , soma and dendrites in the intermediate EPL (Fig. 2A); and T_i , soma in

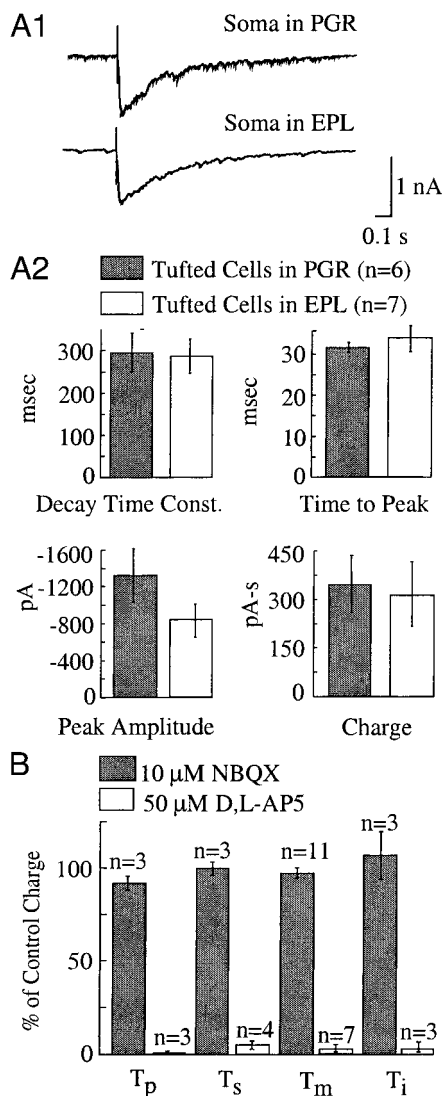


FIG. 3. The characteristics of reciprocal IPSCs were similar for different tufted cell subtypes. *A1*: representative reciprocal IPSCs in a tufted cell in the PGR (*top*) and a tufted cell in the EPL (*bottom*) showed a similar timecourse. *A2*: the decay time constants, time-to-peak, peak amplitude, and total charge were not statistically different for the tufted cell subtypes. For this analysis, tufted cells in all layers of the EPL were pooled. *B*: the relative sensitivity of the reciprocal IPSCs to AP5 and NBQX were also indistinguishable between subtypes. Tufted cells were subtyped based on the location of their soma. T_p , tufted cell in PGR; T_s , tufted cell in superficial zone of EPL; T_m , tufted cell in intermediate zone of EPL; T_i , tufted cell in the deep zone of EPL.

internal portion of the EPL with dendrites in intermediate EPL. In addition, there is at least one morphologically distinct subtype in the PGR (Fig. 2*B*) that is characterized by a single large primary dendrite that projects to a single glomerulus and branches repeatedly within it. Secondary dendrites are rare on PGR tufted cells (Pinching and Powell 1971a), thus inhibitory input must be largely from periglomerular cells, rather than granule cells.

Dendrodendritic IPSCs generated in tufted cells with somata in the EPL (Fig. 3*A1*, *top*) shared similar characteristics to those generated in tufted cells located within the PGR (Fig. 3*A1*, *bottom*). The IPSC decay time constant, time-to-peak, peak amplitude, and IPSC charge were similar for both groups as shown in Fig. 3*A2*. D,L-AP5 (50 μM) completely and re-

versibly abolished the dendrodendritic IPSCs in tufted cells in the periglomerular region and in all zones of the EPL. In contrast, NBQX (10 μM) had no effect (Fig. 3*B*). Thus despite the differences in morphology, all types of tufted cells generate dendrodendritic inhibition with similar receptor pharmacology and kinetics.

Spatial extent of lateral inhibition in tufted cells is less than mitral cells

Our results demonstrate that the general features of dendrodendritic inhibition are similar in mitral and in tufted cells. However, morphological differences, such as the longer secondary dendrites of mitral cells, could affect the extent of lateral inhibition. Hence, we compared the spatial extent of lateral inhibition in mitral cells with that of tufted cells in the intermediate EPL. A bipolar electrode was used to stimulate individual glomeruli at varying lateral distances (ΔL) from the test cell (Fig. 4*A1*). Under our conditions, the bipolar electrode was expected to directly activate the primary dendrites of principal cells within an underlying glomerulus. Because the primary dendrites of principal cells project only to a single glomerulus (Scott and Harrison 1991), lateral movement of the stimulating electrode can be used to quantify the spatial extent of lateral inhibition. As shown for an intermediate tufted cell (T_m) in Fig. 4*A2*, an IPSC generated by stimulation at a lateral separation (ΔL) of 250 μm was markedly smaller than at the control location ($\Delta L = 0$ μm). The relative degree of lateral inhibition in intermediate tufted cells (T_m) was less than mitral cells for all distances examined (Fig. 4, *B* and *C*). Inhibition in tufted cells was completely eliminated at $\Delta L \approx 400$ μm, while inhibition in mitral cells was approximately half-maximal at the same distance (Fig. 4*B*). For all intervals (100–400 μm, binwidth 100 μm), the extent of lateral inhibition in tufted cells was significantly less than that of mitral cells (Fig. 4*C*).

DISCUSSION

NMDA receptor dependence is a general property of dendrodendritic inhibition in the olfactory bulb

Previous reports have demonstrated an unusual dependence of mitral cell dendrodendritic inhibition on NMDA receptor activity in granule cells (Isaacson and Strowbridge 1998; Schoppa et al. 1998). Our results indicate that inhibition in tufted cells shares this property regardless of their morphology or location. Mitral and tufted cells receive inhibitory input from granule and periglomerular cells. Direct recordings from granule cells have demonstrated that excitatory postsynaptic currents (EPSCs) from single mitral cells are conventional in that they have both AMPA and NMDA components, but that the AMPA receptors act primarily to facilitate the depolarization necessary to relieve magnesium block of NMDA receptors. Both the long duration of the NMDA receptor-mediated EPSC as well as its calcium permeability appear to contribute to the release of GABA at dendrodendritic synapses in the bulb (Chen et al. 2000; Halabisky et al. 2000; Schoppa and Westbrook 1999).

Although we did not examine EPSCs in periglomerular (PG) cells evoked by stimulation of single tufted cells, PG cells also express NMDA receptor subunits (Giustetto et al. 1997). Thus we expect that tufted cells also drive the activation of NMDA

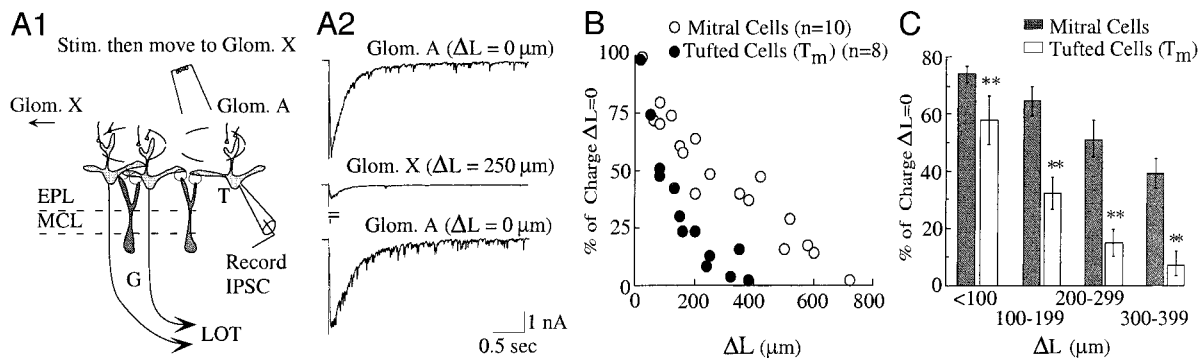


FIG. 4. The spatial extent of lateral inhibition in tufted cells was significantly less than mitral cells. *A1*: bipolar electrode stimulation of a single glomerulus triggered both a reciprocal IPSC as well as a lateral component arising from the activation of neighboring mitral/tufted cells. Lateral movement of the stimulation electrode was used to assess the spatial extent of lateral inhibition. *A2*: an IPSC in a tufted cell in the intermediate EPL was evoked by stimulating the glomerulus to which its primary dendrite projected (Glom. A). However, only a small IPSC was recorded when the stimulating electrode was moved $250 \mu\text{m}$ laterally to an adjacent glomerulus (Glom. X). On return to Glom. A, the IPSC amplitude was unchanged, indicating stability of the recording. *B*: the spatial extent of lateral inhibition in tufted cells ($n = 8$) was less than that of mitral cells ($n = 10$). *C*: at all distance intervals (binwidth, $100 \mu\text{m}$), the magnitude of inhibition in intermediate tufted cells was significantly less than mitral cells (ANOVA analysis). The stimulation artifact was blanked for the current trace ($\Delta L = 250$) as indicated by the "equals" sign.

receptors on these interneurons, leading to GABA release. As for mitral cells, stimulation of only a single tufted cell was sufficient in the absence of extracellular magnesium to evoke a dendrodendritic IPSC. In physiological magnesium, it is expected that stronger stimulation such as activation of many mitral or tufted cells by olfactory nerve activity will be required to depolarize the principal cell sufficiently to activate recurrent and lateral inhibition. Our recordings were performed in slices from rat pups (*P10–P14*). However, a similar pattern of NMDA receptor dependence has been observed in young adult rats using *c-fos* mRNA expression as a measure of cell activity (Schoppa et al. 1998). In those experiments, pretreatment with MK-801 increased *c-fos* mRNA expression in mitral cells consistent with their disinhibition. Close examination also revealed increased cellular activity in scattered large cells throughout the EPL and in PGR, suggesting that there was simultaneous disinhibition of tufted cells.

NMDA receptors are also present on mitral cell dendrites and contribute an autoexcitatory response that may influence the excitability of the mitral cell dendrite as well as resulting interneuronal activity (Isaacson 1999; Nicoll and Jahr 1982). We have also recorded autoexcitatory responses in tufted cells in the EPL (Christie, unpublished observation), providing further evidence that the organization of synaptic glutamate receptors is common to both mitral and tufted cells.

Morphological differences between classes of principal cells have functional consequences on signal processing

Although morphological differences between subtypes of interneurons (Kosaka et al. 1998; Mori et al. 1983; Orona et al. 1983) as well as principal cells in the olfactory bulb have been long recognized, the functional consequences of this cellular diversity remains poorly understood. In our experiments, tufted cells located in the PGR, whose dendrodendritic synapses are limited to PG cells (Pinching and Powell 1971b), were not functionally distinct from tufted cells in the EPL that contact PG cells and granule cells (Mori et al. 1983; Orona et al. 1983). Tufted cells in the EPL, while similar in overall morphology to mitral cells, have shorter secondary dendrites (Mori et al. 1983;

Orona et al. 1984), which might predict differences in lateral inhibition. Consistent with this idea, we found that the spatial extent of lateral inhibition in tufted cells located in the intermediate zone of the EPL was less than mitral cells. Secondary dendrites of tufted cells in superficial zones of the EPL are even shorter than those in deeper zones (Mori et al. 1983; Orona et al. 1984). Thus the spatial extent of lateral inhibition may be even less in superficial tufted cells than in the tufted cells in the intermediate EPL. We were not able to explore this issue using direct glomerular stimulation because of the likelihood of electrical artifacts in superficial tufted cells adjacent to the stimulator. Our results suggest that the extent of lateral inhibition of intermediate tufted cells is local, extending for several glomeruli ($\approx 400 \mu\text{m}$), whereas the extent of lateral inhibition of mitral cells extends more broadly ($\approx 750 \mu\text{m}$). Our experiments were performed in magnesium-free solutions that enhance NMDA receptor responses. However, lateral inhibition is also present in mitral cells in physiological extracellular magnesium, although the spatial extent of lateral inhibition is somewhat reduced (Schoppa, unpublished observation).

The precise spatial map of odorant receptors onto glomeruli in the bulb is thought to provide the basis for the odorant code. However, lateral inhibition is likely to be important in tuning of the glomerular map. Several lines of evidence suggest that local interglomerular interactions mediated by tufted cells could occur. For example, odorant receptors that respond to similar odorants are highly homologous (Malnic et al. 1999). Likewise, olfactory receptor neurons that express highly related odorant receptors appear to project their axons to glomeruli that are in close proximity (Tsuboi et al. 1999). Consistent with active local inhibitory interactions, neighboring principal cells that respond to *n*-aliphatic aldehydes are often inhibited by aldehydes whose aliphatic chain is one or more carbon shorter (Yokoi et al. 1995). Such issues are presumably important in odor detection and discrimination as odorants activate multiple glomeruli (Mori et al. 1999; Rubin and Katz 1999) to generate the combinatorial code that constitutes a perceived odor (Malnic et al. 1999).

This work was supported by National Institute of Neurological Disorders and Stroke Grant NS-26494.

REFERENCES

- CAJAL RS. *Histologie du Système Nerveux de l'Homme et des Vertébrés. Tome 2*. Madrid: Instituto Ramón y Cajal, 1911.
- CHEN WR, XIONG W, AND SHEPHERD GM. Analysis of relations between NMDA receptors and GABA release at olfactory bulb reciprocal synapses. *Neuron* 25: 625–633, 2000.
- EZEH PI, WELLIS DP, AND SCOTT JW. Organization of inhibition in the rat olfactory bulb external plexiform layer. *J Neurophysiol* 70: 263–274, 1993.
- GIUSTETTO M, BOVOLIN P, FASOLO A, BONINO M, CANTINO D, AND SASSO-POGNETTO M. Glutamate receptors in the olfactory bulb synaptic circuitry: heterogeneity and synaptic localization of *N*-methyl-D-aspartate receptor subunit 1 and AMPA receptor subunit 1. *Neuroscience* 76: 787–798, 1997.
- HALABISKY B, FRIEDMAN P, RADOJICIC M, AND STROWBRIDGE BW. Calcium influx through NMDA receptors directly evokes GABA release in olfactory bulb granule cells. *J Neurosci* 20: 5124–5134, 2000.
- ISAACSON JS. Glutamate spillover mediates excitatory transmission in the rat olfactory bulb. *Neuron* 23: 377–384, 1999.
- ISAACSON JS AND STROWBRIDGE BW. Olfactory reciprocal synapses: dendritic signaling in the CNS. *Neuron* 20: 749–761, 1998.
- KOSAKA K, TOIDA K, AIKA Y, AND KOSAKA T. How simple is the organization of the olfactory glomerulus?: the heterogeneity of so-called periglomerular cells. *Neurosci Res* 30: 101–110, 1998.
- MACRIDES F AND SCHNEIDER SP. Laminar organization of mitral and tufted cells in the main olfactory bulb of the adult hamster. *J Comp Neurol* 208: 419–430, 1982.
- MALNIC B, HIRONO J, SATO T, AND BUCK LB. Combinatorial receptor codes for odors. *Cell* 96: 713–723, 1999.
- MORI K, KISHI K, AND OJIMA H. Distributions of dendrites of mitral, displaced mitral, tufted, and granule cells in the rabbit olfactory bulb. *J Comp Neurol* 219: 339–355, 1983.
- MORI K, NAGAO H, AND YOSHIHARA Y. The olfactory bulb: coding and processing of odor molecule information. *Science* 286: 711–715, 1999.
- MORI K AND TAKAGI SF. An intracellular study of dendrodendritic inhibitory synapses on mitral cells in the rabbit olfactory bulb. *J Physiol (Lond)* 279: 569–588, 1978.
- NICOLL RA AND JAHR CE. Self-excitation of olfactory bulb neurones. *Nature* 296: 441–444, 1982.
- ORONA E, RAINER EC, AND SCOTT JW. Dendritic and axonal organization of mitral and tufted cells in the rat olfactory bulb. *J Comp Neurol* 226: 346–356, 1984.
- ORONA E, SCOTT JW, AND RAINER EC. Different granule cell populations innervate superficial and deep regions of the external plexiform layer in rat olfactory bulb. *J Comp Neurol* 217: 227–237, 1983.
- PINCHING AJ AND POWELL TPS. The neuron types of the glomerular layer of the olfactory bulb. *J Cell Sci* 9: 305–345, 1971a.
- PINCHING AJ AND POWELL TPS. The neuropil of the glomeruli of the olfactory bulb. *J Cell Sci* 9: 347–377, 1971b.
- PRICE JL AND POWELL TP. The morphology of the granule cells of the olfactory bulb. *J Cell Sci* 7: 91–123, 1970a.
- PRICE JL AND POWELL TP. The synaptology of the granule cells of the olfactory bulb. *J Cell Sci* 7: 125–155, 1970b.
- RUBIN BD AND KATZ LC. Optical imaging of odorant representations in the mammalian olfactory bulb. *Neuron* 23: 499–511, 1999.
- SCHOPPA NE, KINZIE JM, SAHARA Y, SEGERSON TP, AND WESTBROOK GL. Dendrodendritic inhibition in the olfactory bulb is driven by NMDA receptors. *J Neurosci* 18: 6790–6802, 1998.
- SCHOPPA NE AND WESTBROOK GL. Regulation of synaptic timing in the olfactory bulb by an A-type potassium current. *Nature Neurosci* 2: 1106–1113, 1999.
- SCOTT JW AND HARRISON TA. *Neurobiology of Taste and Smell*. Malabar, FL: Krieger, 1991.
- TSUBOI A, YOSHIHARA S, YAMAZAKI N, KASAI H, ASAI-TSUBOI H, KOMATSU M, SERIZAWA S, ISHII T, MATSUDA Y, NAGAWA F, AND SAKANO H. Olfactory neurons expressing closely linked and homologous odorant receptor genes tend to project their axons to neighboring glomeruli on the olfactory bulb. *J Neurosci* 19: 8409–8418, 1999.
- VASSAR R, CHAO SK, SITCHERAN R, NUNEZ JM, VOSSHALL LB, AND AXEL R. Topographic organization of sensory projections to the olfactory bulb. *Cell* 79: 981–991, 1994.
- YOKOI M, MORI K, AND NAKANISHI S. Refinement of odor molecule tuning by dendrodendritic synaptic inhibition in the olfactory bulb. *Proc Natl Acad Sci USA* 92: 3371–3375, 1995.